ISSN: 1410-8917
e-ISSN: 2597-9914

Jurnal Kimia Sains dan Aplikasi 27 (10) (2024): 477-484

Jurnal Kimia Sains dan Aplikasi
Journal of Scientific and Applied Chemistry

Journal homepage: http://ejournal.undip.ac.id/index.php/ksa

Enhanced Antibacterial Efficacy of Ag(I), Cu(II), and Zn(II) Modified Sodalite Zeolite Against *Escherichia coli* and *Staphylococcus aureus*

Sriatun [1,*], Khairini Pertiwi [1], Choiril Azmiyawati [1], Mukhammad Asy'ari [1], Damar Nurwahyu Bima [1], Nor Aida Zubir [2]

[1] Chemistry Department, Faculty of Sciences and Mathematics, Diponegoro University, Jl. Prof. Soedarto, SH., Tembalang, Semarang, Indonesia
[2] School of Chemical Engineering, College of Engineering, Universiti Teknologi MARA, Cawangan Pulau Pinang, Permatang Pauh, Pulau Pinang, 13500, Malaysia

* Corresponding author: sriatun@live.undip.ac.id

https://doi.org/10.14710/jksa.27.10.477-484

Article Info

Article history:

Received: 07th August 2024
Revised: 24th October 2024
Accepted: 28th October 2024
Online: 30th October 2024

Keywords:
sodalite; zeolite; antibacterial; disk diffusion; well diffusion

Abstract

Sodalite zeolite modified with metal ions Ag^+, Cu^{2+}, Cu^{2+}, and Zn^{2+} was successfully synthesized and evaluated for antibacterial activity. The research aims to obtain silver, copper, and zinc metal-modified sodalite separately and determine their antibacterial activity on *Escherichia coli* and *Staphylococcus aureus* bacteria. Sodalite zeolite was synthesized using ludox and sodium aluminate through hydrothermal methods, ensuring uniform crystal growth and optimal crystallinity, as confirmed by X-ray diffraction (XRD) analysis. The average particle sizes of the modified zeolites were determined to be 54.9 nm for Ag-Zeolite, 37.2 nm for Cu-Zeolite, and 28.56 nm for Zn-Zeolite, with structural changes observed through alterations in peak intensity. Scanning Electron Microscopy - Energy Dispersive X-ray (SEM-EDX) analysis showed no significant change in the zeolite's morphology. In addition, the EDX results showed the presence of Ag (3.15%), Cu (3%), and Zn (2.41%) metals indicating successful ion exchange. Antibacterial assays revealed that Cu-Zeolite demonstrated superior efficacy inhibition zones against *Escherichia coli* (14.04±1.26) and *Staphylococcus aureus* (20.74±0.48), highlighting its potential as an antimicrobial agent. The mechanism of action involved the controlled release of metal ions, disrupting bacterial cell membranes and metabolic processes. Notably, Cu^{2+} ions exhibited the strongest antibacterial properties due to their smaller ionic radius and higher electronegativity than Ag^+ and Zn^{2+}. This research underscores the promising applications of metal-ion-modified sodalite zeolite in medical and environmental contexts.

1. Introduction

Developing materials capable of inhibiting microbial growth is very interesting in the scientific field. This is because of its various applications, such as water filter systems, textiles, and medicines. Recently, much attention has been paid to a reliable and more affordable type of antibacterial, namely modified zeolite-based components [1]. Zeolite is a microporous aluminosilicate mineral generally used as an adsorbent, commercial catalyst, and cation exchanger. One of the factors that influences the type of zeolite is the ratio between silica and alumina, where this ratio will affect the physical properties of the resulting zeolite [2].

Sodalite is a synthesized zeolite with a low Si/Al ratio. Sodalite is known as a host molecule material in other synthesized zeolite framework structures, such as type A zeolite and faujasite [3]. The hydrothermal method is one method that is often used to synthesize zeolites [4]. The hydrothermal method is a method that does not require high costs and has easy stages in making zeolites and nanomaterials. Another advantage is that it can produce nanoparticle crystals at low temperatures and make the nanoparticles evenly dispersed [5].

Zeolite itself lacks antibacterial properties. However, it gains antibacterial capabilities when modified with specific metal ions, making zeolites a highly effective material for antibacterial applications. Zeolite modification can be carried out through the process of exchanging Na^+ ions in the zeolite with other metals as antibacterial agents. Antimicrobial metals include silver, copper, zinc, mercury, lead, nickel, and cadmium [6]. Silver has a broad spectrum as an antimicrobial agent with low toxicity to humans [7]. High copper levels in cells can cause damage to membrane integrity [8]. Zinc is also widely used as an antimicrobial agent and has been widely used as an inhibitor of cariogenic bacteria in teeth [9].

Several studies on using zeolite as an antibacterial material have been carried out previously. Yao *et al.* [10] carried out an antibacterial test of zeolite Li *et al.* [11] conducted an antibacterial test on zeolite modified with Ag^+ ions and obtained a minimum inhibitory concentration against *Escherichia coli* bacteria of 9.17 mg/L, while for *Staphylococcus aureus* bacteria, it was 12.50 mg/L. Milenkovic *et al.* [12] conducted an antibacterial test of zeolite A modified with Cu^{2+}, Zn^{2+}, and Ag^+ ions against *Escherichia coli* bacteria and found that Ag-zeolite had the best inhibitory ability.

Based on this explanation, this research aims to obtain synthesized zeolite sodalite nanoparticle type with a low Si/Al ratio modified with metal ions (Cu^{2+}, Zn^{2+}, Ag^+) and determine the antibacterial ability of synthesized zeolite modified by Cu^{2+}, Zn^{2+}, Ag^+ ions, using the disc diffusion and well diffusion methods against *Escherichia coli* and *Staphylococcus aureus* bacteria. This research introduces the novel use of zeolite loaded with various metals, including Ag, Cu, and Zn, for antibacterial applications. The combination of these metals on a zeolite framework represents an innovative approach, offering enhanced antibacterial properties that distinguish this study from existing research in the field.

2. Experimental

2.1. Materials and Tools

LUDOX HS-40 ($SiO_2.5H_2O$) (Sigma-Aldrich), sodium aluminate ($Na_2O.Al_2O_3$) (Sigma-Aldrich), sodium hydroxide (NaOH) (Merck), distilled water, silver nitrate ($AgNO_3$) (Merck), copper (II) nitrate trihydrate ($Cu(NO_3)_2.3H_2O$) (Merck), zinc nitrate hexahydrate ($Zn(NO_3)_2.6H_2O$) (Sigma-Aldrich), *Escherichia coli* (*E. coli*) bacteria, *Staphylococcus aureus* (*S. aureus*) bacteria, ethanol 70% (Merck), nutrient agar (Merck), nutrient broth (Merck), chloramphenicol (CHL, Kimia Farma).

Glassware (Pyrex), magnetic stirrer (Cimarec), oven (Binder ed-53), analytical balance (Ohaus), inoculation needle, cork borer, spirit burner, petri dish (Anumbra), spreader, micropipette (Thermo Finnpipette), incubator, laminar air flow (LAF) (E-Scientific), orbital shaker (Thermo MaxQ-2000), UV-Vis spectrophotometer (Shimadzu UV-1201), X-ray diffraction (XRD) (Shimadzu XRD-7000), and scanning electron microscope – energy dispersive X-ray (SEM-EDX) (Jeol JSM-6510LA).

2.2. Synthesis of Zeolite

The synthesis of zeolite in this research was based on previous studies by Demirci *et al.* [13] and Osonio and Vasquez [14]. Zeolite was synthesized hydrothermally with a Si/Al ratio of 1. To prepare a 1.69 M NaOH solution, 17.45 g of NaOH pellets were dissolved in 249 mL of distilled water. Afterward, 16.4 g of $Na_2O.Al_2O_3$ was added to the NaOH solution and stirred until fully dissolved, resulting in a 0.75 M $Na_2O.Al_2O_3$ solution. Then, 11.6 mL of Ludox was added to this solution and stirred until homogeneous. The hydrothermal process was conducted in an oven at 150°C for 24 hours, followed by an aging process at room temperature for 24 hours. The mixture was then filtered, washed until neutral, and dried. The synthesized zeolite solids were characterized using SEM-EDX and XRD.

2.3. Modification of Synthesized Zeolite

The enrichment of silver, copper, and zinc metals into zeolite was based on the methods of Cui *et al.* [15] and Septommy *et al.* [16]. A 2 g sample of synthesized zeolite was combined with 20 mL of 0.05 M $AgNO_3$ solution. After 5 hours, the mixture was filtered, and the solid was washed with distilled water and dried at 80°C for 3 hours, yielding Ag^+–Zeolite.

The same procedure was followed to produce Cu^{2+}–Zeolite and Zn^{2+}–Zeolite by adding 0.05 M $Cu(NO_3)_2$ and 0.05 M $Zn(NO_3)_2$ solutions, respectively. The modified zeolite samples were then characterized using SEM-EDX and XRD.

2.4. Antibacterial Activity Test of Modified Zeolite

The initial step involved preparing the MacFarland Standard Solution, nutrient agar, and nutrient broth media. *E. coli* and *S. aureus* bacteria were rejuvenated, and bacterial suspensions were prepared. The antibacterial test was conducted using the disc diffusion method, with Whatman filter paper No. 42 as the disc material. Paper discs dipped in the sample solution were placed on agar media inoculated with 0.1 mL of either *S. aureus* or *E. coli* bacterial suspension. Incubation was carried out at 37°C for 24 hours. Following incubation, the diameter of the inhibition zone was measured with a caliper to obtain the average clear zone diameter. CHL was used as a positive control, while distilled water was a negative control. Control antibacterial tests were also performed on 0.5 M $AgNO_3$, 0.5 M $Cu(NO_3)_2.3H_2O$, and $Zn(NO_3)_3.6H_3O$ solutions.

3. Results and Discussion

3.1. Synthesis and Modification of Zeolite

Synthesized zeolite can be prepared from materials that serve as sources of silica and alumina, such as ludox ($SiO_2.5H_2O$) and sodium aluminate ($Na_2O.Al_2O_3$). Ludox, a colloidal form of silica, is chosen as the silica source due to its high concentration of silanol functional groups and large surface area. These properties make ludox an effective binder for metals, oxides, and other silica-based materials, while its reactive functional groups enhance its performance in the synthesis process [17].

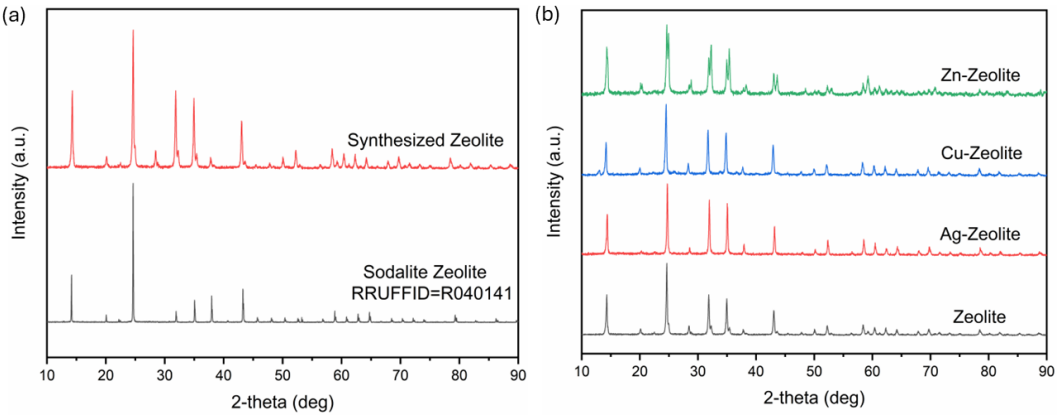

Figure 1. Diffractogram of (a) the standard and synthesized zeolite before modification and (b) zeolite after modification

The synthesis of zeolite in this context is carried out using the hydrothermal method, which involves combining the precursors in a molar ratio of $Na_2O{\cdot}Al_2O_3$: SiO_2: 150 H_2O. This method promotes the formation of zeolite crystals under controlled conditions. The hydrothermal process is essential for ensuring uniform and complete crystal growth, while the aging process enhances the crystallinity of the zeolite, optimizing crystal formation.

Zeolite formation occurs in alkaline conditions, as pH is crucial in determining the species of silicates and aluminates present in the solution. Specifically, the $Al(OH)_4^-$ anion is the primary zeolite-forming aluminate species, with its concentration reaching optimal levels at pH ≥ 9. Similarly, silicate species, such as $Si(OH)_4$ and the Si^{4+} cation, exhibit their highest concentrations at pH > 12 [18]. Additionally, sodium ions (Na^+) act as balancing cations within the zeolite structure. Since the Al^{3+} ions in the zeolite framework generate excess negative charges, Na^+ ions are necessary to neutralize these charges, thereby stabilizing the overall structure [19]. The interaction between sodium aluminate and ludox leads to the polymerization of aluminate and silicate species, resulting in the formation of a white aluminosilicate gel. This gel indicates a strong interaction between the aluminate and silicate components, which is critical for the successful synthesis of zeolite [20].

The hydrothermal process aims to achieve uniform and optimal crystal growth. The aging process enhances the zeolite's crystallinity, maximizing crystal formation. During the hydrothermal method, the alumina silicate mixture undergoes rearrangement, leading to a more regular structure and crystal formation [21]. The formed crystals consist of bonds between Si–O–Al atoms, with oxygen atoms as links [22]. Different metal cations can be introduced to create functionalized zeolite materials. For example, Ag^+-Zeolite (Ag-Zeolite) is synthesized by adding a silver nitrate ($AgNO_3$) solution to synthesized zeolite. Similarly, Zn^{2+}-Zeolite (Zn-Zeolite) is produced by incorporating zinc nitrate ($Zn(NO_3)_2.6H_2O$), and Cu^{2+}-Zeolite (Cu-Zeolite) is obtained by adding copper nitrate ($Cu(NO_3)_2$). These metal precursors donate Ag^+, Zn^{2+}, and Cu^{2+} cations, which replace Na^+ ions in the zeolite framework.

Table 1. The 2θ values of synthesized zeolite and standard zeolite sodalite

2θ value of sodalite zeolite standard (°)	Intensity	2θ synthesized zeolite (°)	Intensity of synthesized zeolite
14.14	53.18	14.34	53
20.05	15.24	20.16	8
24.62	100	24.65	100
28.51	19.8	28.47	12
31.96	98.07	31.86	58
35.10	77.6	34.95	53
38.02	13.65	37.81	7
43.35	19.89	43.05	37

3.2. Characteristics of Zeolite and Modified Zeolite

3.2.1. Crystal Structures of Zeolite and Modified Zeolite

XRD analysis is used to determine the crystal phase or type of the zeolite and its degree of crystallinity. The XRD diffractograms of the synthesized zeolite, both before and after modification with Ag(I), Cu(II), and Zn(II) metal ions, are presented in Figure 1. As shown in Figure 1a, the synthesized zeolite exhibits a crystalline phase characteristic of the sodalite type. The average crystal size of the unmodified zeolite is approximately 47.6 nm, classifying it as sodalite nanoparticles (NPs) due to its nanoscale dimensions and structural properties. The mean crystal size was calculated using the Debye-Scherrer equation.

As depicted in Figure 1b and summarized in Table 1, the diffractogram of the unmodified synthesized zeolite shows distinct peaks associated with sodalite zeolite at 2θ values of 14.34°, 20.16°, 24.65°, 28.47°, 31.86°, 34.95°, 37.81°, and 43.05°. These peaks confirm the crystalline structure of the sodalite phase (RRUFFID=R040141). After modification with metal ions, the average particle sizes of the resulting zeolite composites were found to be 54.9 nm for Ag-Zeolite, 37.2 nm for Cu-Zeolite, and 28.56 nm for Zn-Zeolite.

Table 2. Results of EDX analysis of synthesized sodalite zeolite before and after modification

Elemental	Massa (%)			
	Zeolite Sodalite	Ag-Zeolite	Cu-Zeolite	Zn-Zeolite
Si	10.59	8.24	11.48	8.57
Al	11.61	9.54	12.49	9.55
Na	11.67	9.07	10.29	8.76
Ag	-	3.15	-	-
Cu	-	-	3.00	-
Zn	-	-	-	2.41
O	66.11	70.01	62.74	70.72
Ratio Si/Al	1.1	1.16	1.09	1.11

The incorporation of Ag^+, Cu^{2+}, and Zn^{2+} ions results in a noticeable reduction in the intensity of several 2θ peaks in the diffractogram. This decrease in peak intensity is likely due to interference from these metal ions, as the reflected X-rays from the crystal planes are partially blocked by the Ag^+, Cu^{2+}, and Zn^{2+} ions attached to the zeolite structure. Additionally, modification with Cu^{2+} ions introduces a new peak at 2θ = 12.93°, which was not present in the unmodified zeolite. Similarly, modification with Zn^{2+} ions leads to the appearance of a new peak at 2θ = 53.02°, further confirming the structural changes induced by these metal ions.

3.2.2. Surface Morphology of Zeolite and Modified Zeolite

SEM-EDX analysis was performed to examine the surface morphology and elemental composition of the synthesized zeolite. The results, presented in Figure 2, show that the synthesized zeolite exhibits a flat, clustered, spherical crystal structure characteristic of sodalite. After modification with metal ions such as Ag^+, Cu^{2+}, and Zn^{2+}, the morphology of the sodalite remains largely unchanged, suggesting that introducing these metal ions does not significantly alter the crystal structure. SEM-EDX analysis further confirms that the modification process does not substantially affect the overall morphology, indicating the stability of the sodalite crystal structure. Elemental composition analysis via EDX reveals the primary constituents of both the unmodified and modified sodalite zeolite, as summarized in Table 2, showing the presence of elements from both the sodalite framework and the introduced metal ions. These findings confirm successful modification without structural disruption.

As shown in Table 2, the synthesized sodalite zeolite exhibits a Si/Al ratio ranging from 1.09 to 1.16, indicating a balanced structural composition typical of sodalite-type zeolites. The presence of Ag, Cu, and Zn elements in the modified samples confirms the successful incorporation of Ag^+, Cu^{2+}, and Zn^{2+} ions into the sodalite framework. A notable decrease in the sodium (Na) mass percentage after modification suggests that Na^+ ions were exchanged with the introduced Ag^+, Cu^{2+}, and Zn^{2+} ions during the ion exchange process. Specifically, Ag-Zeolite contains 3.15% Ag by mass, Cu-Zeolite contains 3% Cu, and Zn-Zeolite contains 2.41% Zn.

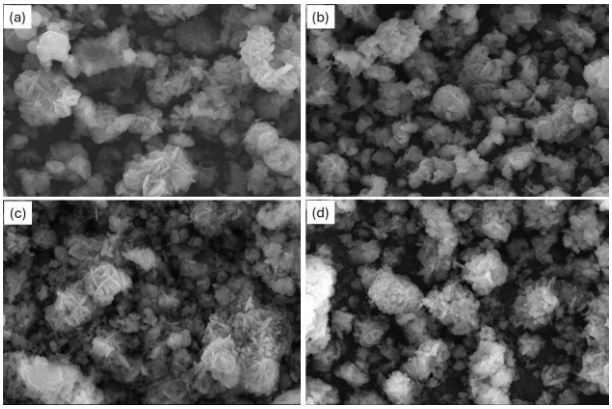

Figure 2. Morphology images of (a) sodalite zeolite before modification, (b) Ag-Zeolite, (c) Cu-Zeolite, (d) Zn-Zeolite at 3,000× magnification

The higher concentration of Ag^+ ions in the sodalite structure, compared to Cu^{2+} and Zn^{2+} ions, can be attributed to the ease with which Ag^+ is exchanged for Na^+ ions. Despite Ag^+ having a relatively larger ionic radius (127 pm) than Cu^{2+} and Zn^{2+}, its size is closer to that of Na^+ ions, which have an ionic radius of 116 pm. This size similarity facilitates a smoother ion-exchange process [23]. Additionally, the identical +1 charge of Ag^+ and Na^+ (or other M^+ ions) enhances the exchange, minimizing the energetic barriers typically associated with charge imbalance during ion substitution [24]. These factors—the similarity in ionic size and identical charge—allow Ag^+ ions to replace Na^+ ions more efficiently in the sodalite framework than Cu^{2+} and Zn^{2+}, whose differing charges and ionic radii make the exchange process less favorable.

3.3. Antibacterial Activity of Zeolite and Modified Zeolites

The antibacterial activity of sodalite zeolite modified with Ag(I), Cu(II), and Zn(II) metal ions was evaluated against *E. coli* (a gram-negative bacterium) and *S. aureus* (a gram-positive bacterium). The bacterial cultures were standardized to the McFarland 0.5 standard, corresponding to approximately 1.5×10^8 CFU/mL, ensuring consistent bacterial colony numbers across all tests. CHL, a well-known antibiotic, was used as the positive control, while distilled water was the negative control. Additionally, 0.05 M solutions of $AgNO_3$, $Cu(NO_3)_2$, and $Zn(NO_3)_2$ were used as control samples for their respective metal ions.

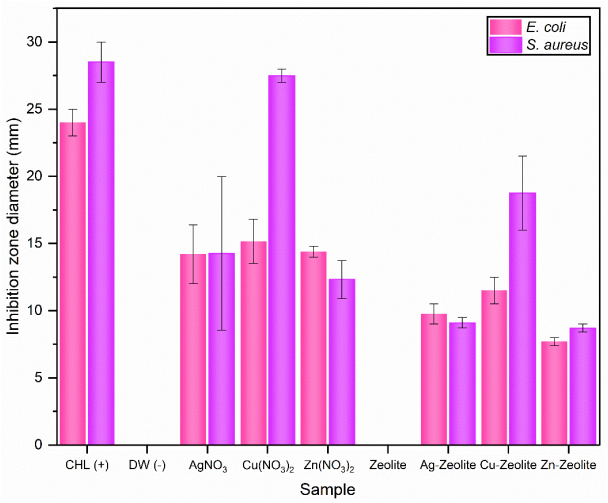

Figure 3. Antibacterial activity using the disc diffusion method against *E. coli* and *S. aureus* bacteria

The disk diffusion method was employed to assess antibacterial activity based on the principle that a disk saturated with an antibacterial agent diffuses radially through the agar medium, creating a clear zone of bacterial inhibition around the disk [25]. After incubation, a clear zone forms around the disk if the compound effectively inhibits bacterial growth. Figure 3 indicates that CHL, as the positive control, exhibited the largest clear zone diameter, demonstrating its potent antibacterial effect on both *E. coli* and *S. aureus*.

Distilled water, as the negative control, and the unmodified zeolite did not produce any clear zones, confirming their lack of antibacterial properties. Among the modified zeolites, Cu-Zeolite exhibited the largest average clear zone diameter for *E. coli* and *S. aureus*, outperforming Ag-Zeolite and Zn-Zeolite. Similarly, in the control samples, the $Cu(NO_3)_2$ solution produced the largest clear zone diameter compared to $AgNO_3$ and $Zn(NO_3)_2$ solutions, indicating that copper ions exert the strongest antibacterial effect. The well-diffusion method operates similarly to the disk diffusion method. In this approach, the antimicrobial agent is introduced into wells created on an agar medium inoculated with the test microorganism. As the antimicrobial agent diffuses through the agar, it inhibits the growth of the microbes in the surrounding area. The size of the clear zone around the well indicates the efficacy of the antimicrobial agent in inhibiting microbial growth [26].

Figure 4 shows that CHL, the positive control, had the largest clear zone, confirming its strong antibacterial effect against *E. coli* and *S. aureus*. The results from the well-diffusion method also reveal that neither distilled water nor unmodified zeolite generated a clear zone, indicating that they lack antibacterial properties and are ineffective in inhibiting the growth of *E. coli* and *S. aureus*. Among the modified zeolites, Cu-Zeolite exhibited the strongest antibacterial activity, producing the largest clear zone in both bacteria, surpassing the effects of Ag-Zeolite and Zn-Zeolite. Similarly, the $Cu(NO_3)_2$ solution also produced the largest clear zone than $AgNO_3$ and $Zn(NO_3)_2$, further confirming the superior antibacterial effectiveness of copper ions in this context.

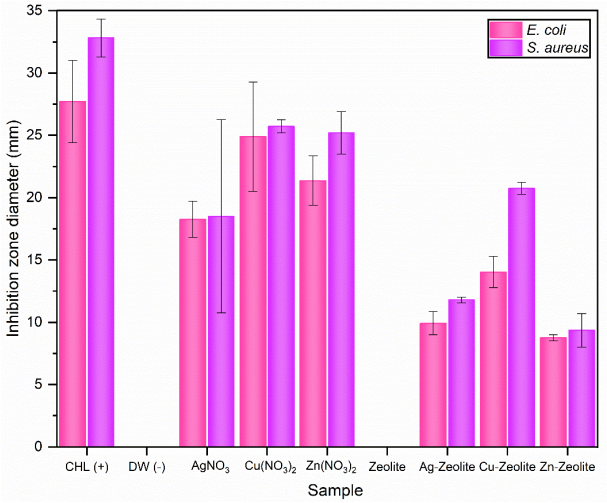

Figure 4. Antibacterial activity using the well-diffusion method against *E. coli* and *S. aureus* bacteria

Ag-Zeolite, Cu-Zeolite, and Zn-Zeolite exhibit lower antibacterial activity compared to their respective control solutions ($AgNO_3$, $Cu(NO_3)_2$, and $Zn(NO_3)_2$). This disparity arises because the control solutions can directly interact with the bacterial cells, resulting in larger clear zones. In contrast, when metal ions are loaded into zeolite, they are released more gradually, leading to slower interaction with the bacteria. Zeolites modified with antibacterial metal ions, such as Ag^+, Cu^{2+}, or Zn^{2+}, can still inhibit bacterial growth, but through a different mechanism. This mechanism involves the controlled release of the metal ions from the zeolite framework, contributing to the antibacterial action.

The slow release of Ag^+, Cu^{2+}, and Zn^{2+} ions from the zeolite allows these ions to interact with the negatively charged bacterial cell membranes. This interaction disrupts the integrity of the bacterial cell walls in both *E. coli* (gram-negative) and *S. aureus* (gram-positive), causing cell wall damage [27]. Additionally, Cu^{2+} ions can penetrate the bacterial cell protoplasm and form Cu-proteinate compounds, which interfere with the cell's metabolic processes, ultimately inhibiting its ability to function and reproduce [28].

In this study, the antibacterial mechanism appears to be primarily attributed to the release of Ag^+, Cu^{2+}, and Zn^{2+} ions from the zeolite surface, as the bacterial cells are too large to enter the pores of the zeolite. Both *E. coli* and *S. aureus* bacteria adhere to the surface of the zeolite, where they interact with the released metal ions. This interaction is crucial to the observed antibacterial activity, as the ions bind to the bacteria's cell membranes, causing damage through the oligodynamic effect [29].

The release of Ag^+, Cu^{2+}, and Zn^{2+} ions from the zeolite is facilitated by their interactions with the sulfhydryl (R-SH) groups on the bacterial cell membranes. The oligodynamic effect, which refers to the ability of small amounts of metal ions to exert a potent antimicrobial effect, is activated during this process. Metal ions, such as Ag^+, Cu^{2+}, and Zn^{2+}, exhibit antibacterial properties by coagulating proteins and reacting with sulfhydryl groups, rendering these groups inactive [30].

According to the Hard and Soft Acid Base (HSAB) theory, the sulfhydryl group (R-SH) is classified as a soft base, while Ag^+ is categorized as a soft acid [31]. Soft acids, such as Ag^+, have a small ionic radius, low oxidation state, and strong polarization, allowing them to bind effectively with soft bases like sulfhydryl groups. In contrast, Cu^{2+} and Zn^{2+} ions are considered borderline acids but still exhibit significant antibacterial properties through similar interactions [32].

The number of metal ions embedded in zeolite significantly influences its antibacterial effectiveness in inhibiting the growth of *E. coli* and *S. aureus* bacteria. Higher concentrations of Ag^+, Cu^{2+}, and Zn^{2+} ions enhance the antibacterial activity. This occurs due to the electrostatic interaction between the positively charged metal ions and the negatively charged bacterial cell membrane, which creates a strong attraction between them [33]. As more Ag^+, Cu^{2+}, and Zn^{2+} ions are released from the zeolite, more bacterial cells are targeted and killed, forming larger clear zones during antibacterial tests. The antibacterial mechanism of metal ions involves their interaction with critical bacterial components such as the peptidoglycan cell wall, bacterial DNA, and bacterial proteins.

The interaction between metal ions and the peptidoglycan cell wall and plasma membrane results in the disruption of these structures, ultimately leading to cell lysis [34]. Metal ions can also bind to bacterial DNA, interfering with its ability to replicate. By binding to DNA bases, the metal ions inhibit bacterial reproduction through the process of binary fission [35]. Additionally, metal ions can interfere with protein synthesis by interacting with bacterial ribosomes (specifically the 70S ribosomes), thereby disrupting protein production and compromising the integrity of the plasma membrane [36].

Among the metal-ion-modified zeolites, sodalite zeolite modified with Cu^{2+} ions exhibited the most potent antibacterial activity, producing the largest clear zones. This can be explained by the size and electronegativity of the Cu^{2+} ions compared to Ag^+ and Zn^{2+} ions. The smaller ionic radius of Cu^{2+} (72 pm) allows for stronger interactions with bacterial cell components compared to the larger radii of Ag^+ (113 pm) and Zn^{2+} (83 pm) ions [37].

This smaller size enhances the attraction between Cu^{2+} ions and the negatively charged bacterial cell membrane. Additionally, Cu^{2+} has a relatively high electronegativity of 1.90, contributing to its strong binding with the bacterial membrane. In contrast, Ag^+ ions, despite having a similar electronegativity (1.93), are more prone to reduction [38]. The Ag^+ ion easily loses its antimicrobial activity due to its tendency to undergo reduction from Ag^+ to Ag^0, which diminishes its antibacterial properties. Zn^{2+} ions, with a lower electronegativity of 1.65, exhibit weaker antibacterial activity compared to Cu^{2+} ions [39, 40].

The experimental results demonstrate that sodalite zeolite loaded with metal ions, particularly Cu^{2+} exhibits strong antibacterial properties. Notably, these metal-ion-loaded zeolites show greater efficacy against *S. aureus* (Gram-positive bacteria) than *E. coli* (Gram-negative bacteria). The difference in susceptibility can be attributed to the structural complexity of the bacterial cell walls. Gram-positive bacteria, like *S. aureus*, have a simpler cell wall structure, making them more vulnerable to metal ion interactions. In contrast, Gram-negative bacteria, such as *E. coli*, possess an additional outer membrane composed of lipopolysaccharides, which act as a barrier to prevent the penetration of metal ions. This protective layer contributes to the reduced sensitivity of Gram-negative bacteria to metal-ion-based antibacterial agents [41, 42]. Thus, the combination of smaller ionic radius, higher electronegativity, and efficient interaction with bacterial cells makes Cu-modified zeolite a particularly effective antimicrobial agent, outperforming its Ag and Zn^{2+} counterparts.

4. Conclusion

This study investigated the synthesis, modification, and antibacterial activity of sodalite zeolite loaded with metal ions—Ag^+, Cu^{2+}, and Zn^{2+}. The zeolite was synthesized using ludox and sodium aluminate via hydrothermal methods, achieving uniform crystal growth and optimal crystallinity, confirmed by XRD analysis. Post-modification, Ag-Zeolite, Cu-Zeolite, and Zn-Zeolite exhibited average particle sizes of 54.9 nm, 37.2 nm, and 28.56 nm, respectively, with changes in peak intensity indicating structural alterations. SEM-EDX analysis showed no significant change in the zeolite's morphology, confirming successful ion exchange with elemental analysis. Antibacterial efficacy was evaluated against *E. coli* and *S. aureus* using the disk diffusion method, revealing that Cu-Zeolite exhibited the greatest antibacterial activity. The mechanism primarily involved gradually releasing metal ions, disrupting bacterial cell membranes and metabolic processes. Cu^{2+} ions, with their smaller ionic radius and higher electronegativity, were the most effective against both bacterial strains, outperforming Ag^+ and Zn^{2+}. This research highlights the potential of metal-ion-modified sodalite zeolite as an effective antimicrobial agent, suggesting avenues for further applications in medical and environmental fields.

Acknowledgment

We sincerely thank the Dean of the Faculty of Science and Mathematics at UNDIP for supporting this research through funding for the 2023 fiscal year, as outlined in contract No. 21/UN7.F8/PP/II/2023.

References

[1] Jesús Isaías De León Ramirez, Víctor Alfredo Reyes Villegas, Ruben D. Cadena-Nava, Elizabeth Loredo-Garcia, Fernando Chávez-Rivas, Verónica González-Torres, Vitalii Petranovskii, Antimicrobial activity of the LTA zeolite modified by zinc species, *Microporous and Mesoporous Materials*, 380, (2024), 113295 https://doi.org/10.1016/j.micromeso.2024.113295

[2] Barbara Liguori, Paolo Aprea, Bruno de Gennaro, Fabio Iucolano, Abner Colella, Domenico Caputo, Pozzolanic Activity of Zeolites: The Role of Si/Al Ratio, *Materials*, 12, 24, (2019), 4231 https://doi.org/10.3390/ma12244231

[3] Natalia Kordala, Mirosław Wyszkowski, Zeolite Properties, Methods of Synthesis, and Selected Applications, *Molecules*, 29, 5, (2024), 1069 https://doi.org/10.3390/molecules29051069

[4] David Längauer, Vladimír Čablík, Slavomír Hredzák, Anton Zubrik, Marek Matik, Zuzana Danková, Preparation of Synthetic Zeolites from Coal Fly Ash by Hydrothermal Synthesis, *Materials*, 14, 5, (2021), 1267 https://doi.org/10.3390/ma14051267

[5] Aleksander Ejsmont, Joanna Goscianska, Hydrothermal Synthesis of ZnO Superstructures with Controlled Morphology via Temperature and pH Optimization, *Materials*, 16, 4, (2023), 1641 https://doi.org/10.3390/ma16041641

[6] G. M. Wangi, P. W. Olupot, J. K. Byaruhanga, R. N. Kulabako, A Review for Potential Applications of Zeolite-Based Nanocomposites in Removal of Heavy Metals and *Escherichia coli* from Drinking Water, *Nanotechnologies in Russia*, 15, 11, (2020), 686-700 https://doi.org/10.1134/S1995078020060221

[7] Elena Sánchez-López, Daniela Gomes, Gerard Esteruelas, Lorena Bonilla, Ana Laura Lopez-Machado, Ruth Galindo, Amanda Cano, Marta Espina, Miren Ettcheto, Antoni Camins, Amélia M. Silva, Alessandra Durazzo, Antonello Santini, Maria L. Garcia, Eliana B. Souto, Metal-Based Nanoparticles as Antimicrobial Agents: An Overview, *Nanomaterials*, 10, 2, (2020), 292 https://doi.org/10.3390/nano10020292

[8] Grażyna Gromadzka, Beata Tarnacka, Anna Flaga, Agata Adamczyk, Copper Dyshomeostasis in Neurodegenerative Diseases—Therapeutic Implications, *International Journal of Molecular Sciences*, 21, 23, (2020), 9259 https://doi.org/10.3390/ijms21239259

[9] Mohammad Tariqur Rahman, Ashfaque Hossain, Chew Hooi Pin, Noor Azlin Yahya, Zinc and Metallothionein in the Development and Progression of Dental Caries, *Biological Trace Element Research*, 187, (2019), 51-58 https://doi.org/10.1007/s12011-018-1369-z

[10] Guangyuan Yao, Jingjing Lei, Wanzhong Zhang, Caihong Yu, Zhiming Sun, Shuilin Zheng, Sridhar Komarneni, Antimicrobial activity of X zeolite exchanged with Cu^{2+} and Zn^{2+} on *Escherichia coli* and *Staphylococcus aureus*, *Environmental Science and Pollution Research*, 26, 3, (2019), 2782-2793 https://doi.org/10.1007/s11356-018-3750-z

[11] Yanzhi Li, Qiqing Tan, Tingting Li, Yaozong Tan, Ganjun Yang, Yong Huang, Enhui Xing, Xuanwei Zhang, Qiang Chen, Ultrasmall Ag clusters in situ encapsulated into Silicalite-1 zeolite with controlled release behavior and enhanced antibacterial activity, *Microporous and Mesoporous Materials*, 330, (2022), 111617 https://doi.org/10.1016/j.micromeso.2021.111617

[12] Jelena Milenkovic, Jasna Hrenovic, Danka Matijasevic, Miomir Niksic, Nevenka Rajic, Bactericidal activity of Cu-, Zn-, and Ag-containing zeolites toward *Escherichia coli* isolates, *Environmental Science and Pollution Research*, 24, 25, (2017), 20273-20281 https://doi.org/10.1007/s11356-017-9643-8

[13] Selami Demirci, Zeynep Ustaoğlu, Gonca Altın Yılmazer, Fikrettin Sahin, Nurcan Baç, Antimicrobial Properties of Zeolite-X and Zeolite-A Ion-Exchanged with Silver, Copper, and Zinc Against a Broad Range of Microorganisms, *Applied Biochemistry and Biotechnology*, 172, 3, (2014), 1652-1662 https://doi.org/10.1007/s12010-013-0647-7

[14] Airah P. Osonio, Magdaleno R. Vasquez, Plasma-assisted reduction of silver ions impregnated into a natural zeolite framework, *Applied Surface Science*, 432, (2018), 156-162 https://doi.org/10.1016/j.apsusc.2017.09.076

[15] Hu Cui, Yang Ou, Lixia Wang, Baixing Yan, Yingxin Li, Meiwen Bao, Critical passivation mechanisms on heavy metals during aerobic composting with different grain-size zeolite, *Journal of Hazardous Materials*, 406, (2021), 124313 https://doi.org/10.1016/j.jhazmat.2020.124313

[16] Catur Septommy, Sa'adah Nikmatus, Binti Mu'arofah, The effect of natural Zeolite (Ag-Zeolite) modified with silver against the inhibition of *Candida albican*, *Journal of Syiah Kuala Dentistry Society*, 5, 2, (2020), 56-60 https://doi.org/10.24815/jds.v5i2.20013

[17] Jonas G. Croissant, Kimberly S. Butler, Jeffrey I. Zink, C. Jeffrey Brinker, Synthetic amorphous silica nanoparticles: toxicity, biomedical and environmental implications, *Nature Reviews Materials*, 5, 12, (2020), 886-909 https://doi.org/10.1038/s41578-020-0230-0

[18] Zully Matamoros-Veloza, Juan Carlos Rendon-Angeles, Kazumichi Yanagisawa, Tadaharu Ueda, Kongjun Zhu, Benjamin Moreno-Perez, Preparation of Silicon Hydroxyapatite Nanopowders under Microwave-Assisted Hydrothermal Method, *Nanomaterials*, 11, 6, (2021), 1548 https://doi.org/10.3390/nano11061548

[19] Daniele Malferrari, Fabrizio Bernini, Dario Di Giuseppe, Valentina Scognamiglio, Alessandro F. Gualtieri, Al-Substituted Tobermorites: An Effective Cation Exchanger Synthesized from "End-of-Waste" Materials, *ACS Omega*, 7, 2, (2022), 1694-1702 https://doi.org/10.1021/acsomega.1c04193

[20] Dongshuai Hou, Mengqi Sun, Muhan Wang, Xiaomei Wan, Zheng Chen, Xinpeng Wang, Yue Zhang, Pan Wang, Molecular Insight into the Formation and Fracture Process of Sodium Aluminosilicate Hydrate Gels, *The Journal of Physical Chemistry C*, 127, 31, (2023), 15542-15555 https://doi.org/10.1021/acs.jpcc.3c02632

[21] Ying Zhang, Baiyu Huang, Maryam K. Mardkhe, Brian F. Woodfield, Thermal and hydrothermal stability of pure and silica-doped mesoporous aluminas, *Microporous and Mesoporous Materials*, 284, (2019), 60-68 https://doi.org/10.1016/j.micromeso.2019.04.005

[22] Aslam Kunhi Mohamed, Pinelopi Moutzouri, Pierrick Berruyer, Brennan J. Walder, Jirawan Siramanont, Maya Harris, Mattia Negroni, Sandra C. Galmarini, Stephen C. Parker, Karen L. Scrivener, Lyndon Emsley, Paul Bowen, The Atomic-Level Structure of Cementitious Calcium Aluminate Silicate Hydrate, *Journal of the American Chemical Society*, 142, 25, (2020), 11060-11071 https://doi.org/10.1021/jacs.0c02988

[23] Sreejith M. Nair, Afaq Ahmad, Effect of Cation Substitution on Fast Ag^+ Ion Conductivity in Ag_2CdI_4,

Journal of Physics and Chemistry of Solids, 58, 2, (1997), 331-333 https://doi.org/10.1016/S0022-3697(96)00116-3

[24] Liliya I. Shamova, Grigory A. Shamov, Igor S. Antipin, Alexandr I. Konovalov, Modeling K^+ and Ag^+ Complexation by Thiacalix[4]arene Amides Using DFT: The Role of Intramolecular Hydrogen Bonding, *The Journal of Physical Chemistry A*, 113, 19, (2009), 5691-5699 https://doi.org/10.1021/jp810947g

[25] Rémy A. Bonnin, Cécile Emeraud, Agnès B. Jousset, Thierry Naas, Laurent Dortet, Comparison of disk diffusion, MIC test strip and broth microdilution methods for cefiderocol susceptibility testing on carbapenem-resistant enterobacterales, *Clinical Microbiology and Infection*, 28, 8, (2022), 1156.E1151-1156.E1155 https://doi.org/10.1016/j.cmi.2022.04.013

[26] Mareshah Abers, Sydney Schroeder, Linna Goelz, Adrienne Sulser, Tiffany St. Rose, Keely Puchalski, Jeffrey Langland, Antimicrobial activity of the volatile substances from essential oils, *BMC Complementary Medicine and Therapies*, 21, 1, (2021), 124 https://doi.org/10.1186/s12906-021-03285-3

[27] Jixing Cui, Rezwana Yeasmin, Yuanyuan Shao, Haiping Zhang, Hui Zhang, Jesse Zhu, Fabrication of Ag^+, Cu^{2+}, and Zn^{2+} Ternary Ion-Exchanged Zeolite as an Antimicrobial Agent in Powder Coating, *Industrial & Engineering Chemistry Research*, 59, 2, (2020), 751-762 https://doi.org/10.1021/acs.iecr.9b05338

[28] Xiaoli Qi, Ningfei Shen, Aya Al Othman, Alexandre Mezentsev, Anastasia Permyakova, Zhihao Yu, Mathilde Lepoitevin, Christian Serre, Mikhail Durymanov, Metal-Organic Framework-Based Nanomedicines for the Treatment of Intracellular Bacterial Infections, *Pharmaceutics*, 15, 5, (2023), 1521 https://doi.org/10.3390/pharmaceutics15051521

[29] Inocente Rodríguez-Iznaga, Vitalii Petranovskii, Felipe F. Castillón-Barraza, Sergio Fuentes-Moyado, Fernando Chávez-Rivas, Alexey Pestryakov, Mordenite-Supported Ag^+-Cu^{2+}-Zn^{2+} Trimetallic System: A Variety of Nanospecies Obtained via Thermal Reduction in Hydrogen Followed by Cooling in an Air or Hydrogen Atmosphere, *Materials*, 16, 1, (2023), 221 https://doi.org/10.3390/ma16010221

[30] Homa Ghasemi, Nidal Abu-Zahra, Umair Baig, Nadeem Baig, Abdul Waheed, Isam H. Aljundi, Synergistic integration of copper-functionalization and smart release mechanisms for enhanced bacterial inactivation on polyethersulfone membranes, *Journal of Environmental Chemical Engineering*, 11, 5, (2023), 110408 https://doi.org/10.1016/j.jece.2023.110408

[31] Lei Wang, Cunzhi Zhang, Hui He, Hongxiang Zhu, Wei Guo, Shile Zhou, Shuangfei Wang, Joe R. Zhao, Jian Zhang, Cellulose-based colorimetric sensor with N, S sites for Ag^+ detection, *International Journal of Biological Macromolecules*, 163, (2020), 593-602 https://doi.org/10.1016/j.ijbiomac.2020.07.018

[32] Aliyu M. Hamisu, Azhar Ariffin, Arief C. Wibowo, Cation exchange in metal-organic frameworks (MOFs): The hard-soft acid-base (HSAB) principle appraisal, *Inorganica Chimica Acta*, 511, (2020), 119801 https://doi.org/10.1016/j.ica.2020.119801

[33] Yael N. Slavin, Jason Asnis, Urs O. Häfeli, Horacio Bach, Metal nanoparticles: understanding the mechanisms behind antibacterial activity, *Journal of Nanobiotechnology*, 15, (2017), 65 https://doi.org/10.1186/s12951-017-0308-z

[34] Maria Godoy-Gallardo, Ulrich Eckhard, Luis M. Delgado, Yolanda J. D. de Roo Puente, Mireia Hoyos-Nogués, F. Javier Gil, Roman A. Perez, Antibacterial approaches in tissue engineering using metal ions and nanoparticles: From mechanisms to applications, *Bioactive Materials*, 6, 12, (2021), 4470-4490 https://doi.org/10.1016/j.bioactmat.2021.04.033

[35] Zhenle Cao, Muhammad Shahidul Islam, Jared Sisler, Kam C. Tam, Antimicrobial Assay of Metal Ions Using Yeast and Its Relevance to Food Preservation, *ACS Food Science & Technology*, 4, 6, (2024), 1444-1451 https://doi.org/10.1021/acsfoodscitech.4c00079

[36] Natalia Shcherbik, Dimitri G. Pestov, The Impact of Oxidative Stress on Ribosomes: From Injury to Regulation, *Cells*, 8, 11, (2019), 1379 https://doi.org/10.3390/cells8111379

[37] Mihaela Homocianu, Anton Airinei, Alina Mirela Ipate, Corneliu Hamciuc, Spectroscopic Recognition of Metal Ions and Non-Linear Optical (NLO) Properties of Some Fluorinated Poly(1,3,4-Oxadiazole-Ether)s, *Chemosensors*, 10, 5, (2022), 183 https://doi.org/10.3390/chemosensors10050183

[38] Ru Zhou, Courtney Calahoo, Yicong Ding, Xu Yang, Carl P. Romao, Lothar Wondraczek, Structural Origin of the Optical Properties of Ag-Doped Fluorophosphate and Sulfophosphate Glasses, *The Journal of Physical Chemistry B*, 125, 2, (2021), 637-656 https://doi.org/10.1021/acs.jpcb.0c09375

[39] Zongbo Zhang, Jin Li, Nan Meng, Shiliang Song, Qingqing Zhu, Dawei Li, Liang Gong, Yan Ding, Rui Zhang, Xiaoxu Shi, Simultaneously-efficient electro-sorption of Pb(Ⅱ), Cu(Ⅱ) and Cd(Ⅱ) by Cu^{2+} modified superactive carbons, *Separation and Purification Technology*, 338, (2024), 126604 https://doi.org/10.1016/j.seppur.2024.126604

[40] Esma Hande Alici, Ahmet T. Bilgiçli, Burak Tüzün, Armağan Günsel, Gulnur Arabaci, M. Nilüfer Yarasir, Alkyl chain modified metalophthalocyanines with enhanced antioxidant-antimicrobial properties by doping Ag^+ and Pd^{2+} ions, *Journal of Molecular Structure*, 1257, (2022), 132634 https://doi.org/10.1016/j.molstruc.2022.132634

[41] Md Masudur Rahman, Asmaul Husna, Hatem A. Elshabrawy, Jahangir Alam, Nurjahan Yasmin Runa, A. T. M. Badruzzaman, Nahid Arjuman Banu, Mohammad Al Mamun, Bashudeb Paul, Shobhan Das, Md Mahfujur Rahman, A. T. M. Mahbub-E-Elahi, Ahmed S. Khairalla, Hossam M. Ashour, Isolation and molecular characterization of multidrug-resistant *Escherichia coli* from chicken meat, *Scientific Reports*, 10, 1, (2020), 21999 https://doi.org/10.1038/s41598-020-78367-2

[42] Nicole P. Giordano, Melina B. Cian, Zachary D. Dalebroux, Outer Membrane Lipid Secretion and the Innate Immune Response to Gram-Negative Bacteria, *Infection and Immunity*, 88, 7, (2020), https://doi.org/10.1128/iai.00920-19